



ELSEVIER

Journal of Controlled Release 42 (1996) 165–173

journal of  
**controlled  
release**

## Modifications induced on stratum corneum structure after in vitro iontophoresis: ATR-FTIR and X-ray scattering studies

Anne Jadoul<sup>a</sup>, Jean Doucet<sup>b</sup>, Dominique Durand<sup>b</sup>, Véronique Prémat<sup>a,\*</sup>

<sup>a</sup>*Université Catholique de Louvain, Ecole de Pharmacie, Unité de Pharmacie Galénique, Av. E. Mounier, 73/20, 1200, Brussels, Belgium*

<sup>b</sup>*Université de Paris-Sud, LURE, Bâtiment 209C, 91405, Orsay, France*

Accepted 23 February 1996

### Abstract

The aim of the present work was to investigate stratum corneum (s.c.) structure after prolonged in vitro iontophoresis by two physical techniques: ATR-FTIR and X-ray scattering. ATR-FTIR studies showed that iontophoresis induced an important and reversible increase in the hydration of the outer layers of s.c. but no increase in lipid fluidity could be detected. SAXS (small angle X-ray scattering) of s.c. showed that iontophoresis induced a disorganisation of the lipid layers stacking reversible within a few days. No modification of the intralamellar crystalline packing of lipids nor of keratin were observed by WAXS (wide angle X-ray scattering). From our ATR-FTIR and X-ray scattering observations, it can be assumed that the enhancement in transdermal permeation which characterizes iontophoresis is related to the lipid layer stacking disorganisation.

**Keywords:** Stratum corneum; Skin; Iontophoresis; ATR-FTIR; X-ray Scattering

### 1. Introduction

Stratum corneum (s.c.), the outermost layer of mammalian epidermis, acts as the main barrier for diffusion of substances through the skin. It is composed of corneocytes embedded in lipid domains consisting of alternatively hydrophilic and lipophilic layers. The lipids are arranged in a lamellar phase and at least a part of these lipid bilayers are in a crystalline state. The barrier to permeation was attributed by several authors not only to the interstitial lipid composition but also to their structure as ordered multilayers [1]. However, this barrier is far

from an inert membrane and its diffusion properties can be dramatically altered by interaction with different components. The concept of promoting the transdermal permeation rate of drugs by modifying skin permeability has been applied for many years. Different approaches have been investigated: physical (e.g. iontophoresis), chemical (e.g. coadministration of skin permeation enhancer) or biochemical (e.g. synthesis of bioconvertible prodrugs) [2].

In order to identify the molecular mechanisms underlying barrier function, a number of investigators have utilized physical techniques like X-ray scattering, IR spectroscopy and thermal studies [3]. Since it is assumed that transport takes place mainly through the intercellular route (for review [4]), an effort has been put into elucidation of the lipid lamellar structure and changes in this structure

\*Corresponding author.

notably after treatment with penetration enhancers. The techniques cited above are the most appropriate to explore the architecture of s.c. at the molecular state. For example, Golden et al. [5] observed by spectrometric and calorimetric measurements an increased lipid fluidity following treatment of the stratum with a penetration enhancer. Moreover, the striking parallelism between flux and fluidity measurements suggested that transdermal drug flux may be ultimately related to s.c. lipid structure. Since, analogue studies were extended to other enhancers and did not always show a lipid fluidity enhancement. For example a study on perdeuterated oleic acid did not show fluidization of s.c. lipids. It was postulated consequently that the oleic acid enhancer exists in a separate 'semi-solid' phase distinct from the highly ordered s.c. lipids [6].

Iontophoresis is another approach which has shown potential promise for accomplishing the goals of overcoming the skin's barrier properties, and hence of enhancing the transdermal permeation rate of drugs. It is a method of enhancing and controlling the penetration of ionic drugs through the skin by the application of an external electrical field [7]. The intensive studies of factors affecting the iontophoretic transport led to a greater comprehension and gave prominence to the advantages of electrically facilitated transdermal drug delivery. However, as stated by Ledger [8], modern experimental studies on the iontophoresis effects on skin structure *in vivo* are notable mainly by their scarcity. The different effects of iontophoresis reviewed by Ledger resulted mainly from clinical observations, it was notably erythema, sensations like prickling or outright pain and burns.

Non-invasive techniques were used since in order to elucidate skin integrity after *in vivo* iontophoresis (0.2 mA/cm<sup>2</sup> during 30 min) [9,10]. These studies showed a significant and reversible cutaneous blood flow enhancement (using Laser Doppler flowmeter) and a transient increase in hydration (using ATR-FTIR: attenuated total reflectance-Fourier transform infrared spectroscopy). No alteration in lipids structure could be shown. Recently, FTIR and DSC studies were performed *in vitro* and showed only minimal changes on the lipid cellular matrix: even relatively high current densities did not cause detectable lipid fluidisation nor protein denaturation [11].

The aim of the present work was to investigate s.c. structure after prolonged *in vitro* iontophoresis by

two physical techniques usually used for studies on s.c. properties: ATR-FTIR and X-ray scattering.

## 2. Material and methods

### 2.1. Iontophoresis experiences

Iontophoresis were performed in polycarbonate horizontal cells. Three cm<sup>2</sup> of freshly excised abdominal hairless rat skin (Iops hairless mutant, Iffa Credo, St Germain-les-Arbresles, France) or frozen human skin separated the two compartments of the cell. Human skin samples had to be stored at -80°C due to practical reasons of access to human skin and X-ray source. The anode was introduced in the upper reservoir (1.5 ml), facing the s.c., while the cathode was inserted in the lower compartment (7.5 ml) facing the dermis. Platinum electrodes (Platinum pure, Johnson Matthey, Brussels, Belgium) of 1 cm<sup>2</sup> were connected to a direct current generator. Intensities of 0, 0.33 or 0.5 mA/cm<sup>2</sup> were applied for up to 6 h. The two compartments were filled with phosphate buffer (0.06 M) at pH 7.4 (analysis grade; UCB, RPL, Leuven, Belgium) [12]. The buffer was changed every 1 h 30 min in the upper compartment. However, pH did not decrease below 3. All the solutions were prepared with ultrapure water (Sation 9000, Sation, Barcelona, Spain). After current switch off, the skin was directly analysed by FTIR or the s.c. was isolated for SAXS (Small Angle X-ray Scattering) and WAXS analysis (Wide Angle X-ray Scattering). For ATR-FTIR studies, iontophoresis were compared to samples not exposed to current (control) and freshly excised skin. For X-ray scattering studies, iontophoresis were only compared to control samples (i.e. no-current application).

### 2.2. Stratum corneum isolation

Human and rat epidermis were separated from the dermis by immersing full-thickness skin in a 60°C water bath for 2 min. Epidermal cells were removed from the overlying s.c. by digestion with trypsin 0.1% (type I, Sigma chemical company, Sigma-Aldrich, Bornem, Belgium) in phosphate buffered saline pH 7.4 (HBSS Hank's Balanced Salt w/o phenol red, Gibco BRL, N.V. Life Technologies SA, Merelbeke, Belgium) for 30 min at 37°C. Trypsin

digestion was not necessary for human skin. The resulting s.c. sheets were rinsed with ultrapure water, dried at room temperature and stored in open boxes. Heat separation procedure had to be used to isolate rat s.c., therefore both human and rat skin were submitted to the same procedure. It is possible that thermal treatments induced structure modification but the important point lies in the comparison between the different treatments.

### 2.3. ATR-FTIR

Infra-red spectra were obtained using a Fourier transform infra-red spectroscopy (Perkin Elmer, Spectra Tech, Horizontal ATR 0012-XXX). The application of ATR-FTIR to study the biophysical properties of s.c. has been reported by several authors (see for review [3]). Briefly, in contrast to classic transmission spectroscopy (where the sample intercepts the path of IR beam), in ATR, the sample (in this case the skin and, more precisely, the s.c.), is to bring into contact with an IR transparent crystal (called internal reflectance element or IRE). The geometry of this crystal permits almost total internal reflectance. So, the outer layers of the s.c. can be easily analysed without the need for sample preparation. Furthermore, the FTIR system enables the rapid acquisition and analysis of IR spectra.

All spectra analysed represent an average of 20 scans obtained in 2.8 min with a resolution of  $2\text{ cm}^{-1}$ . The spectra were collected in the wavenumber range  $4000\text{--}1000\text{ cm}^{-1}$  and, for the lipid acyl chain study,  $3350\text{--}2700\text{ cm}^{-1}$ . The internal reflectance element used in this study was a Zinc Selenide trapezoid having  $45^\circ$  entrance and exit faces.

Before analysis, the skin was taken out the cell, gently wiped and directly applied to the crystal, the s.c. (and, more precisely, the stratum disjunctum) facing the IRE. Freshly excised skin were also analysed. The skin was pressed on the crystal with help of a 100 g weight and let at room temperature and humidity during measures. Between measurements, the dermis side of the skin was put on a filter paper soaked with phosphate buffer.

### 2.4. Spectra analysis

The following features of the spectra, and the rationale for their evaluation, were examined as a

function of time (0, 1 and 2 h) after current switch off:

(A) The area under the secondary OH stretching water absorbance at  $2106\text{ cm}^{-1}$ . Potts et al. [13] showed that the water concentration of the s.c. can be quantitatively determined from the absorbance near  $2100\text{ cm}^{-1}$ . Indeed, the area below the absorbance curve is proportional to the amount of the absorbing species. This area was divided by the baseline area which is proportional to the degree of skin contact with IRE. The ratio of areas (or normalized area) then provided an estimation on the relative amount of the absorbing species [14].

The normalized area under the secondary OH band centered around  $2100\text{ cm}^{-1}$  has been used in this study to appraise the s.c. water concentration.

(B) The intensity ratio between amide I (near  $1646\text{ cm}^{-1}$ ) and amide II (near  $1558\text{ cm}^{-1}$ ). The amide I absorbance, due to the carbonyl stretch in the CO-NH group, is strongly increased in the presence of water. This is caused by the strong IR absorption of water near  $1640\text{ cm}^{-1}$  and by changes of the carbonyl absorption under the influence of water. The amide II reflects the amide N-H in plane bending mode and is less influenced by the water peak. So, the intensity ratio amide I/ amide II band allows conclusions to be drawn concerning the water content of the s.c. However, the water influence on both amide I and amide II resonance due to hydrogen bonding, indicates the limitations of this relative hydration measure [15].

(C) The frequency shift and the bandwidth at half-height of the  $\text{-CH}_2\text{-asymmetric}$  stretching absorbance peak observed at approximately  $2920\text{ cm}^{-1}$ . A blue shift could result from an increased number of gauche conformers in the lipid acyl chain (a process called rotamer disordering). The bandwidth at half-height of the  $\text{CH}_2$  stretching absorbance also reflects the relative lipid acyl chain disordering: the greater the acyl chain disorder, i.e. the larger the number of gauche conformers, the greater the bandwidth [16].

### 2.5. X-ray diffraction studies

The X-ray scattering experiments have been carried out using the synchrotron radiation source DCI of LURE (Orsay-France) on station D43. A single bent Si monochromator (111 reflexion) was used to

select the wavelength 1.22 Å and to focalize the beam. The size of the beam was limited by a collimator with a circular aperture of 0.33 mm diameter. Most of the experiments were performed with the incident beam parallel to the plane of the s.c. (parallel geometry) in order to follow the scattering features originating in the lamellar structure of the intercellular lipids which lie parallel to the s.c. plane [17] (SAXS, Small Angle X-ray Scattering). The chosen sample-detector distance corresponds to the range of spacings [180 Å–15 Å]. Some patterns have also been obtained in the perpendicular geometry, at shorter distances (115 mm, corresponding to the range of spacings [30 Å–2.5 Å]), in order to observe in the best conditions the rings due to the regular packing of the lipids within the layers (WAXS, Wide Angle X-ray Scattering). The detection system consists in phosphor image plates which are scanned in two dimensions on the Molecular Dynamics Phosphor Imager 400E with a pixel size of (172 × 172) μm<sup>2</sup>. The comparison between the various patterns has been performed using the intensity profiles (10 pixels width) along the equator (direction perpendicular to the s.c. sheets).

Scattering experiments have been performed on rat and human s.c.. In order to increase the scattering ratio signal/noise, several sheets of s.c. were superposed by folding the sample (disorientation angle smaller than 10°) and gripped vertically. The experiments were carried out in air at room temperature and humidity using about 10 min long exposures. The hydration state can be considered constant for such short durations. For SAXS experiences, only human data are reported in this paper since the modifications of the scattering features due to iontophoresis are almost completely hidden by the effect of hydration on rat s.c. unlike the human s.c. [19] (this difference is probably related to the fact that rat s.c. is thinner than human s.c.). For WAXS experiments, we present data obtained on rat s.c.

The evolution of the patterns has been followed from 30 min after treatment up to 1 week.

Each experiment has been repeated from three up to six times. A common behaviour can be clearly derived from our experiments in spite of some discrepancies, either due to local variations of the s.c. structure or to variations in the efficiency of the treatments.

The scattering pattern analysis is based on the fact that a periodic structure (periodicity  $d$ ) gives rise to a scattering peak in a direction such as the angle  $2\theta$  between the incident beam and the scattered beam is given by Bragg's law:  $\lambda = 2d \sin\theta$  where  $\lambda$  is the wavelength. In the case of a lamellar structure,  $d$  is the thickness of the layers and  $\theta$  is the angle between the incident beam (or scattered) and the plane of the layers.

The s.c. intracellular lipid layers are not perfectly parallel to the sheet's plane; in consequence the scattered intensity is not only localized along a normal direction to the s.c. sheet but along cones, which give rise to rings on the scattering patterns with an intensity maximum along the normal to the s.c. sheets. In WAXS geometry, the scattering rings are isotropic because the s.c. structure do not display an isotropy in its plane.

## 2.6. Statistical analysis

Statistical analysis in FTIR studies were performed using one-way analysis of variance.

## 3. Results

### 3.1. ATR-FTIR

#### 3.1.1. Normalized area under 2106 cm<sup>-1</sup>

The normalized areas were compared for each experiments.

As shown in Fig. 1, iontophoresis induced an increase in the area under 2106 cm<sup>-1</sup> peak as compared to control, which was significant only at time 0 and 1 h with high intensities (0.5 mA/cm<sup>2</sup>). These results suggest that iontophoresis increased hydration in the outer layers of s.c. reversibly.

#### 3.1.2. Amide I and amide II

As seen in Fig. 2, a significant difference in intensity ratio of amide I/amide II was observed until 2 h between 0.5 mA/cm<sup>2</sup> iontophoresis and control. A weaker current intensity (0.33 mA/cm<sup>2</sup>) induced a significant absorbance ratio difference only immediately after current switch off. These results indicate that iontophoresis enhanced s.c. hydration

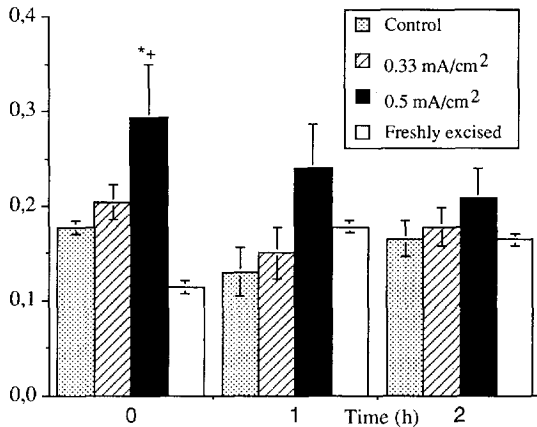


Fig. 1. Normalized area under the secondary O–H stretching band as function of time after current switch off. Iontophoresis were performed 6 h with a current density of 0 (control), 0.33 or 0.5 mA/cm<sup>2</sup> and compared to freshly excised skin. \*  $P < 0.05$  vs freshly excised, +  $P < 0.05$  vs. diffusion.

which was quickly reversible following 0.33 mA/cm<sup>2</sup> iontophoresis.

### 3.1.3. $-CH_2$ -asymmetric stretching peak

The wavenumber shift (Fig. 3) and the bandwidth at half height (data not shown) of the  $-CH_2$ -asymmetric stretching were compared.

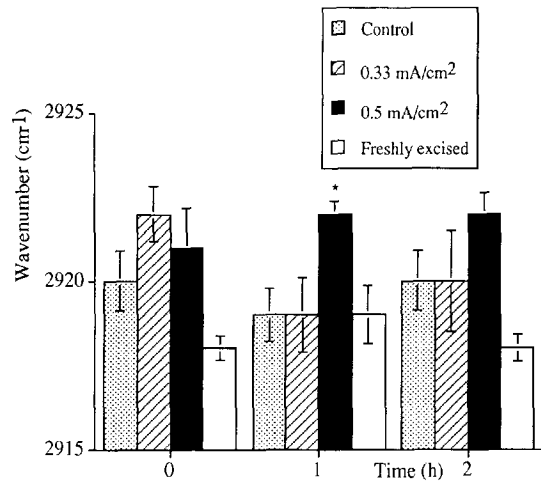


Fig. 3. Position of asymmetric stretching absorbance peak as function of time after current switch off. Iontophoresis were performed 6 h with a current density of 0 (control), 0.33 or 0.5 mA/cm<sup>2</sup> and compared to freshly excised skin. \*  $P < 0.05$  vs freshly excised.

No significant difference was observed between the bandwidths. No significant shift between iontophoresis (even at a current density of 0.5 mA/cm<sup>2</sup>) and control was observed. A weak shift (of few cm<sup>-1</sup>) was observed between iontophoresis at higher density and freshly excised skin but only 2 h after current switch off. This was probably an artefact due to the broad O–H stretching peak from water.

A large amount of water (e.g. after iontophoresis, even 2 h after current switch off) may artifactually influence the apparent position of the s.c. lipid CH<sub>2</sub>-absorbance [17]. To check if this increase in hydration did not modify the stretching vibration of  $-CH_2-$  at 2920 cm<sup>-1</sup>, iontophoresis were performed with buffered D<sub>2</sub>O introduced in both compartments of the cell. No variation in the wavenumber was detected as compared to iontophoresis with buffered H<sub>2</sub>O. Therefore, the shift due to changes in the shape of the O–H peak did not mask a blue shift due to increased alkyl chain mobility. These results indicate that current application does not result in lipid alkyl chain disordering. However, as indicated by Green et al. [8], higher current densities could be localized in pores resulting in an alteration of the structure in this region which is unlikely to be detected using this technique due to the small fractional area involved.

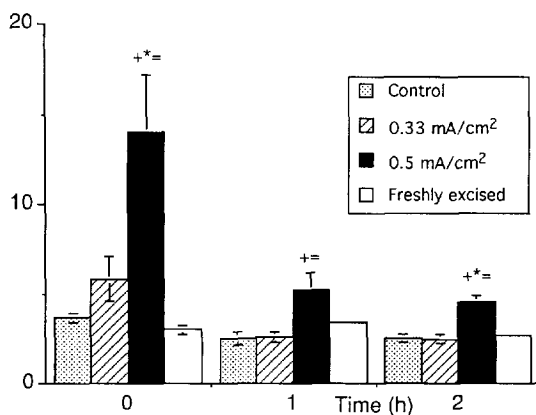


Fig. 2. Intensity ratio of amide I/amide II stretching absorbance as function of time after current switch off. Iontophoresis were performed 6 h with a current density of 0 (control), 0.33 or 0.5 mA/cm<sup>2</sup> and compared to freshly excised skin. \*  $P < 0.05$  vs freshly excised, +  $P < 0.05$  vs. control, =  $P < 0.05$  vs. 0.33 mA/cm<sup>2</sup>.

### 3.2. X-ray diffraction

#### 3.2.1. SAXS

##### Control pattern

The intensity profile (a) on Fig. 4 gives the SAXS intensity profile along the equator of the control sample after 24 h, i.e. to the sample which has been in contact with the solution without application of the electric field.

Two broad peaks were visible around 65 Å and 45 Å. These peaks have been attributed by Garson et al. to two different and independent lamellar structures due to the stacking of lipids; it has been assumed that the signal at 65 Å arises from layers containing a large proportion of ceramides [18]. Nevertheless, our profile differed slightly from those on the following points: (i) we did not observe any thin peak at 40 Å which was attributed to large domains of triglycerides [18]. (ii) our broad ring at 45 Å extended almost along a complete circle instead of being mostly located on the equator; this indicates that the layers which are responsible for the peak did not lie preferentially parallel to the s.c. plane. (iii) our two peaks were slightly broader and less intense than those of Garson et al. [18].

Differences (i) and (ii) were perhaps due to

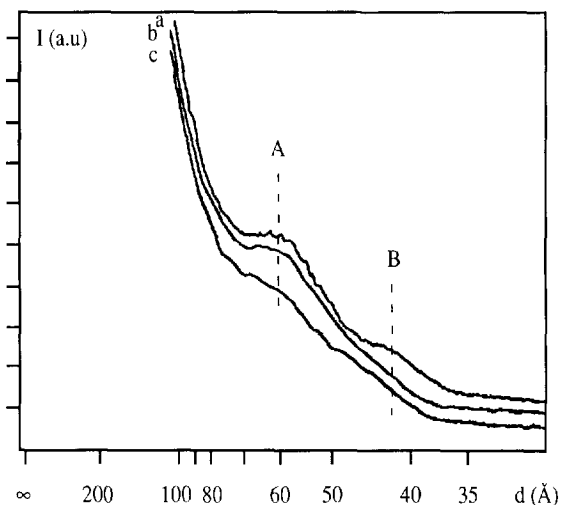


Fig. 4. Scattering intensity profiles along the equator of the three samples about 24 h after current switch off. From top to bottom, the curves correspond to 0 (control; a), 0.33 (b) and 0.5 mA/cm<sup>2</sup> (c) current density applied during 6 h.

slightly different procedures of preparation. We separated the s.c. at 60° whereas it was separated at 37°C by Garson et al. [18].

Difference (iii) could be due to a difference in donor, but it is more probable that it was due to a different water content of the samples. Our control pattern could directly be compared to those of wet s.c. described by Bouwstra et al. [19]. These authors have shown that the pattern of a sample saturated with water (60% w/w) only exhibits one peak at 65 Å, whereas a 40% w/w sample exhibits the two peaks at 65 Å and 45 Å, but less intense and slightly broader than in dry s.c.. After 24 h, our control sample pattern was quite similar to that of a 40% w/w sample.

The interpretation of these observations is that water damages the regular layered stacking of the intercellular lipids.

##### Effect of iontophoresis 0.33 mA/cm<sup>2</sup>

The intensity profile (b) of Fig. 4 corresponds to a 6 h iontophoresis treatment at 0.33 mA/cm<sup>2</sup>. The difference with the control profile was quite obvious. On the 0.33 mA/cm<sup>2</sup> pattern, we noted the vanishing of the 45 Å peak while the 65 Å was unperturbed. This pattern was similar to that of the 60% w/w sample of Bouwstra et al. [19]. The effect of 0.33 mA/cm<sup>2</sup> iontophoresis was to reinforce the damage caused by water to the lipid stacking, or at least to delay their re-ordering.

##### Effect of iontophoresis 0.5 mA/cm<sup>2</sup>

On the pattern of the 0.5 mA/cm<sup>2</sup> iontophoresis sample (Fig. 4c), both the 65 Å and the 45 Å peaks have disappeared. It can be concluded that the layer structure of the two main families of lipids was highly perturbed or even nearly destroyed. Such damage which cannot be induced by water alone has already been observed after permeation enhancer application such as a combination of C12 azones and propylene glycol [20].

##### Evolution with time

Fig. 5 shows the modifications of the scattering intensity profiles as a function of time. Up to about 110 h after iontophoresis, no change was seen on profiles for iontophoretic treatments (curves b and c);

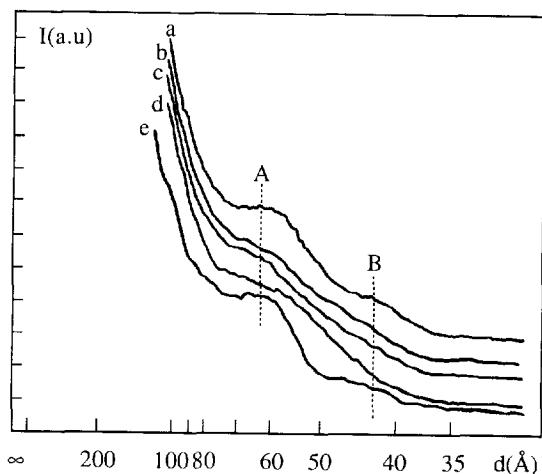


Fig. 5. Evolution of the scattering intensity profile along the equator after 6 h iontophoresis performed at a current density of  $0.5 \text{ mA/cm}^2$ . From top to bottom, the curves correspond to 0 (control); a), 23 h (b), 71 h (c), 144 h (d) and 166 h (e) after current switch off.

then a broad peak appeared (curve d obtained at 140 h) and it finally split after 170 h into the two peaks at about  $65 \text{ \AA}$  and  $45 \text{ \AA}$  which were very similar to the peaks observed for the control sample (curve a). This behaviour was in fact not always so well defined both qualitatively and quantitatively since the return to a state close to the initial one was not always observed within 1 week.

These observations indicated that the lamellar stacking of the lipids which was damaged by iontophoresis displayed a tendency to restore its initial structure after about 1 week at room temperature and humidity. This duration has to be compared to the rather short time (a few hours) which characterizes the control sample.

### 3.2.2. WAXS

Fig. 6 shows the scattering intensity profile of the WAXS patterns in perpendicular geometry. The control sample is identical as those previously published [18,21]. It displays two broad bands, one around  $9.6 \text{ \AA}$  which comes from keratin and the other around  $4.5 \text{ \AA}$  which is due both to keratin and to non-crystallized lipids. The two main diffraction peaks resulting from the crystallized lipids are located at reticular distances  $4.11 \text{ \AA}$  and  $3.75 \text{ \AA}$  (not visible on Fig. 6).

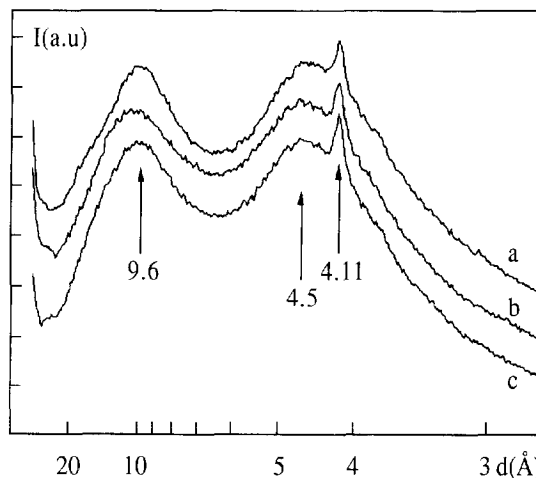


Fig. 6. Scattering intensity profiles in WAXS about 24 h after current switch off. From top to bottom, the curves correspond to control (a),  $0.33 \text{ mA/cm}^2$  (b) and  $0.5 \text{ mA/cm}^2$  (c) current density applied during 6 h.

The patterns corresponding to iontophoresis treatments  $0.33 \text{ mA/cm}^2$  and  $0.5 \text{ mA/cm}^2$  (Fig. 6b and c) were not significantly different from the control sample pattern. This observation proves that the intralamellar molecular stacking of the intercellular lipids is not modified by iontophoresis: the crystalline order is altered neither qualitatively nor quantitatively. No melting of the lipids or keratin modification is particularly observed. This is not surprising since it can be assumed that the intralamellar cohesion is strong, as suggested by the fact that their periodic order is obtained only with the very small number of intracellular bilayers.

## 4. Discussion

The main modification induced by iontophoresis and detected in the infrared spectra of the outer layers of the stratum corneum was an increase in hydration. No lipid chain disordering was observed. These observations confirm the results obtained by other investigators both *in vivo* [9,10] and *in vitro* [11]. Indeed, a previous *in vivo* study showed a transient increase (30 min) in hydration after current application for 30 min at  $0.2 \text{ mA/cm}^2$ . Moreover, in the same study, the fast reversibility of the enhance-

ment in transepidermal water loss values after iontophoresis was explained by an increase in skin hydration rather than by a modification of the barrier function of the entire s.c.. Moreover, this absence of lipid acyl chains disordering could not be explained by a fast recovery of the ordering since the study performed by Clancy et al. [11] *in vitro* and *in situ* showed that, even at relatively high current density, no detectable fluidisation was observed.

X-ray scattering experiments showed that a disorganisation of the lipid regular stacking more or less pronounced was associated with iontophoresis. The application of an electric field had a similar effect on the intercellular lipid structures to that observed for some penetration-enhancing agents (water, chemical substances) [21,22]. It can thus be assumed that this disorganisation could explain the penetration enhancement. This conclusion is physically reasonable since it is well known that the permeation is governed by the density of the molecular packing, which is larger for the periodic ordered structures than for the disordered ones. The application of an electric field in iontophoresis experiments would both favour the damaging of the lamellar lipid stacking and delay its return to the initial state. The other conclusion derived from the X-ray experiments is that the intralamellar packing of the lipids chains remains unchanged by the iontophoresis treatments.

Nevertheless it is possible that other processes which are not detectable by X-ray diffraction may accompany the damaging effects and even play a more important role in the penetration enhancement than these effects, like, for example, the formation of empty channels.

## 5. Conclusion

Our ATR-FTIR and X-ray scattering data showed that iontophoresis induces a disorganisation of the lipid layer stacking and a hydration. It does not induce any modification of the intralamellar crystalline packing of the lipids nor of the molecular conformation. Therefore, it is probable that the enhancement in transdermal delivery could correspond to a loss of the coupling between the intercellular lipid bilayers which could favour the interlamellar diffusion of molecules.

## 6. Acknowledgments

V. Pr at is a senior researcher of the Fonds National de la Recherche Scientifique (Belgium). This work was supported by the Fonds National de la Recherche Scientifique.

## References

- [1] R.O. Potts and M.L. Francoeur, The influence of s.c. morphology on water permeability, *J. Invest. Dermatol.* 96 (1991) 495–499.
- [2] Y.W. Chien, Advances in transdermal systemic drug delivery. *Drugs Future* 13 (1988) 343–362.
- [3] R. Potts, Physical characterization of the stratum corneum: the relationship of mechanical and barrier properties to lipid and protein structure. in: J. Hadgraft and R. Guy (Eds.) *Transdermal Drug Delivery*, Marcel Dekker, New York, 1989, pp. 23–57.
- [4] C. Cullander, What are the pathways of iontophoretic current flow through mammalian skin? *Adv. Drug Del. Rev.* 9 (1992) 119–135.
- [5] G.M. Golden, J.E. McKie and R.O. Potts, Role of stratum corneum lipid fluidity in transdermal drug flux. *J. Pharm. Sci.* 76 (1987) 25–28.
- [6] A. Naik, L. Pechtold, R.O. Potts and R.H. Guy, Mechanisms of skin penetration enhancement, *in vivo*, in man. in: K.R. Brain and V.A. Walters (Eds.) *Prediction Percutaneous Penetration*, Vol. 3b, 1993, pp. 161–165.
- [7] B.H. Sage, Iontophoresis. in: J. Swarbrick and J.C. Boylan (Eds.) *Encyclopedia of Pharmaceutical Technology*, Vol. 8, 1993, pp 217–247.
- [8] P.W. Ledger, Skin biological issues in electrically enhanced transdermal delivery. *Adv. Drug Del. Rev.* 9 (1992) 289–307.
- [9] R.D. Green and J. Hadgraft, FT-IR investigations into the effect of iontophoresis on the skin. in: K.R. Brain and V.A. Walters (Eds.) *Prediction Percutaneous Penetration*, Vol. 3b, 1993, pp. 37–43.
- [10] S. Thysman, D. Van Neste and V. Pr at, Noninvasive investigation of human skin after *in vivo* iontophoresis, *Skin Pharmacol.*, 8 (1995) 229–236.
- [11] M.J. Clancy, J. Corish and O.I. Corrigan, A comparison of the effects of electrical current and penetration enhancers on the properties of human skin using spectroscopic (FTIR) and calorimetric methods. *Int. J. Pharm.* 105 (1994) 47–56.
- [12] S. Thysman, C. Tasset and V. Pr at, Transdermal iontophoresis of fentanyl: delivery and mechanistic analysis. *Int. J. Pharm.* 101 (1994) 105–113.
- [13] R.O. Potts, D.B. Guzek, R.R. Harris and J.E. McKie, A noninvasive, *in vivo* technique to quantitatively measure water concentration of the stratum corneum using attenuated total-reflectance infrared spectroscopy. *Arch Dermatol. Res.* 277 (1985) 489–495.



- [14] P.A. D. Edwardson, M. Walker and C. Breheny, Quantitative FT-IR determination of skin hydration following occlusion with hydrocolloid containing adhesive dressings. *Int. J. Pharm.* 91 (1993) 51–57.
- [15] M. Gloor, G. Hirsch and U. Willebrandt, On the use of infrared spectroscopy for the in vivo measurement of water content of the horny layer after application of dermatologic ointments. *Arch. Dermatol. Res.* 271 (1981) 305–313.
- [16] H.L. Casal and H.H. Mantsch, Polymorphic phase behaviour of phospholipid membranes studied by infrared spectroscopy. *Biochem. Biophys.* 779 (1984) 381–401.
- [17] V.H.W. Mak, R.O. Potts and R.H. Guy, Does hydration affect intercellular lipid organization in the stratum corneum ?. *Pharm. Res.* 8 (1991) 1064–1065.
- [18] J. Garson, J. Doucet, J. Leveque and G. Tsoucaris, Oriented structure in human stratum corneum revealed by X-ray diffraction. *J. Invest. Dermatol.* 96 (1991) 43–49.
- [19] J.A. Bouwstra, G.S. Gooris, J.A. van der Spek and W. Bras, Structural investigations of human stratum corneum by small-angle X-ray scattering. *J. Invest. Dermatol.* 97 (1991) 1005–1012.
- [20] J.A. Bouwstra, M.A. de Vries, G.S. Gooris, W. Bras, J. Brussee and M. Ponc, Thermodynamic and structural aspects of the skin barrier. *J. Control. Release* 15 (1991) 209–220.
- [21] J.A. Bouwstra, G.S. Gooris, M.A. de Vries, J.A. van der Spek and W. Bras, Structure of human stratum corneum as a function of temperature and hydration: a wide angle X-ray diffraction study. *Int. J. Pharm.* 84 (1992) 205–216.
- [22] F. Schückler, J.A. Bouwstra, G.S. Gooris and G. Lee, An X-ray diffraction study of some model stratum corneum lipids containing azone and dodecyl-L-pyroglytamate. *J. Control. Release* 23 (1993) 27–36.